# SUB-WAVELENGTH NANOTEXTURED PLASMONIC SILICON SOLAR CELLS

**P.R. Pudasaini[1*], A. Ayon[1]**
[1]Department of Physics and Astronomy, University of Texas at San Antonio, USA

We report a noble plasmonics silicon solar cells design with the possibility of lower cost and higher efficiency. The proposed solar cells consist of radial p-n junction silicon nanopillars array textured surface in combination with plasmonics metal nanoparticles on its surface. The optical and electrical performances of the nanopillars surface textured silicon solar cells depend on dimensions of the nanopillars. The power conversion efficiency *(PEC)* of the nanopillars textured solar cells with nanopillars height 800nm is found to be 10.7%. Unlike the better optical performance, the electrical performance of nanopillars surface textured solar cells degrades with the increased heights of the pillars beyond 800nm. The *PCE* of the plasmonics metal nanoparticles decorated nanopillars textured solar cells is decreased to 7.31% due to the increased recombination, which suggests for the requirement of advanced passivation of the nanotextured surface.

**Keywords:** Solar cells, plasmonics, optical absorption, power conversion efficiency

## INTRODUCTION

In the recent years, there is large interest in noble solar cells device architectures with the possibility of lower cost, higher efficiency and large scale integration [1, 2] . Light trapping in the solar cells has played an important role in improving the efficiency of the solar cells by allowing weakly absorbed light to go through multiple reflections within the cell. To this end, plasmonics light trapping has been extensively studied both by theoretically and experimentally [3-6]. Plasmonics light trapping has the immense potential to reduce the physical thickness of the solar cells by keeping the optical thickness constant mainly by the two basic phenomenons. Firstly, the metallic nanoparticles can be used as subwavelength scattering element to couple and trap freely propagating light wave in to the substrate. Secondly, the metallic nanoparticles can be used as subwavelength antennas in which the plasmonic near field is coupled to the substrate, increasing its effective cross-section area. Furthermore, radial p-n junction structures composed of vertically aligned nanopillars array attract much attention because they may allow the cell fabrication with the materials having short minority carrier diffusion length by decoupling the light absorption and carrier extraction into orthogonal spatial directions. Radial junction wire array solar cells have experienced significant improvement in the recent years, and different groups have reported that the efficiency of silicon wire array radial junction solar cells are closed to 10% [7, 8] . In this work, we proposed a new solar cells design composed of the plasmon enhanced radial junction silicon nanopillars textured surface via a method with the potential of lower cost.

## EXPERIMENTAL DETAILS

The wafer scale highly ordered silicon nanopillars (SiNP) array was fabricated by metal assisted electroless chemical etching (MAECE) in combination with naosphere lithography (NSL). Four inch p-type silicon (100) wafer with the resistivity of 1-10 Ω-cm was cleaned using Piranha solution (an aqueous solution of 30% $H_2O_2$ and, conc. $H_2SO_4$ in volume ratio of 1:3) at $90^0$C for 10 minutes followed by the strong rinse in DI water and drying by the stream of nitrogen. The wafer is then immersed in RCA solution (as aqueous solution of 30% $H_2O_2$, conc. $NH_4OH$ and, DI water in volume ratio of 1:1:5) at $80^O$C for 30 minutes to obtain a hydrophilic surface. The Polystyrene (PS) nanoparticles aqueous solution was prepared by mixing PS solution (5065B, Duke Scientific, Palo Alto, CA) with Triton X-100 diluted with methanol. The PS particles were spin coated on the silicon surface and then tailored using commercial Barrel etcher. A 40nm of gold (Au) film was deposited on PS coated sample by using commercial table top sputter coater. The honeycomb like Au mask was created by liftoff of PS particles. The periodic SiNP array was fabricated by immersing the sample in the etching solution of HF, $H_2O_2$ and $H_2O$ in the volume ratio of 25:10:75. The mechanism of MAECE can be found elsewhere [9, 10]. The samples were examined by using high resolution scanning electron microscope (Hitachi S-5500). The optical reflectance spectra measurements were performed by using UV-VIS-NIR (Varian cary-5000) spectrometer equipped with integrating spheres.

The spin on dopant (SOD) solution was prepared by sol-gel method, mixing phosphorous pentaoxide ($P_2O_5$), tetraethoxysilane (TEOS), ethanol ($C_2H_5OH$)

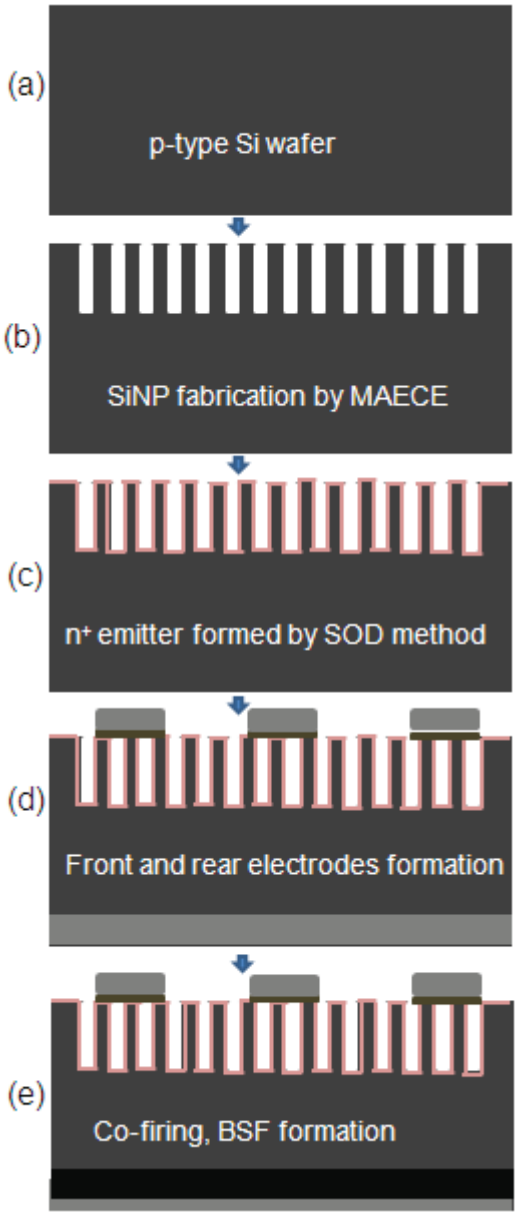


*Fig. 1: Schematic of fabrication processes of radial junction SiNP array textured solar cells. (a) 1-10 ohm-cm p-type CZ silicon wafer, (b) fabrication of SiNP array by MAECE method, (c) radial p-n junction formation by SOD technique, (d) Ni/Ag front and Al back electrode formation, (e) back surface field formation by firing the sample at 750$^0$C for 5 minutes.*

and DI water. The SOD solution was spin coated on the silicon nanopillar array textured surface to form the radial p-n junction by heating the sample at 870$^0$C for 10 minutes. The parasitic layer was then removed by immersing the sample in HF aqueous solution for 120 sec. The front side nickel (80nm) /silver (400nm) fingers like grid electrode was formed by conventional photolithography technique and the rear side aluminum electrode was formed by coating Al paste provided by ferro corporation, California, US. The samples were then fired at 750$^0$C for 5 minutes to form the back surface field (BSF). The fabrication processes of SiNP arrays textured solar cells are shown in figure 1. The nanopillars array was decorated by the Au nanoparticles formed by annealing the thin Au film on the top of the nanopillars at 400$^0$C for 30 minutes. The PV measurement was performed using a solar simulator under AM 1.5G illumination (1000W/m$^2$).

## RESULTS AND DISCUSSION

Fig. 2 shows the SEM micrographs of different steps of NSL technique.

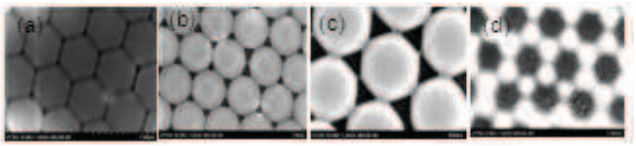


*Fig. 2: The SEM micrographs of different steps of NSL. (a) hexagonal packing of PS nanoparticles (b) tailored PS nanoparticles by $O_2$ plasma (c) Au coated PS nanoparticles (d) honeycomb like gold pattern.*

Fig. 3 shows the SEM micrographs of the SiNP created by the MAECE, immersing the sample in the etching solution for 3 minutes. The etching rate was observed to be 0.4 micron per minute. The dimension of the SiNP array was controlled by the Au mask and the etching time.

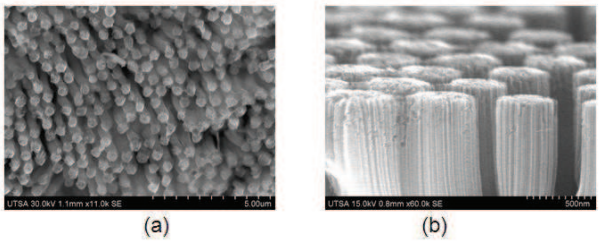


*Fig. 3: The SEM micrographs of SiNP arrays formed by MAECE. (a) tilted planer view (b) cross-sectional view.*

Fig. 4(a) shows the reflectance spectra for the SiNP array for different nanopillar heights H, with the array periodicity of 650nm and diameter 500nm. Ostensibly, the reflectivity decreases with the increase in SiNP heights through the entire range of wavelength. The graph with the red line corresponds

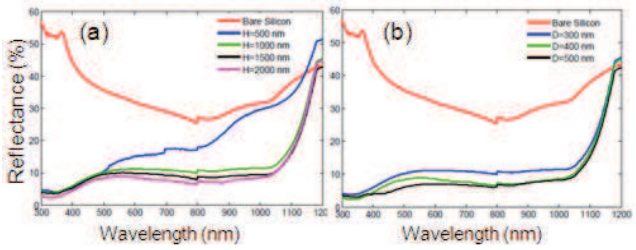


*Fig. 4: Optical reflectance spectra of SiNP array textured surface. (a) for different height with P = 650 nm, H = 500 nm (b) for different diameter with P = 650 nm, H = 2000 nm*

to the reflectivity measurement for bare silicon surface for comparison. We observed, the reflectivity reduces to ~2% (350nm) as the nanopillar height increased to 2000nm (graph with magenta line). The measured reflectance is well below 10% through the entire range of wavelength from 300nm to 1100nm. This is because of improved antireflection effect due to the gradual change in refractive index with the increased height of the nanopillars. Fig. 4(b) depicts the measured reflectance as a function of wavelength for different diameters of the SiNP array with the periodicity 650nm and height 2000nm. Evidently, the measured reflectance decreases with the increase in diameter of the SiNP from 300nm to 500nm except in the short wavelength region. This is because of the presence of higher order diffraction mode with the increased diameter. However, higher energy photons were reflected back with the increase in diameter of the nanopillars as expected.

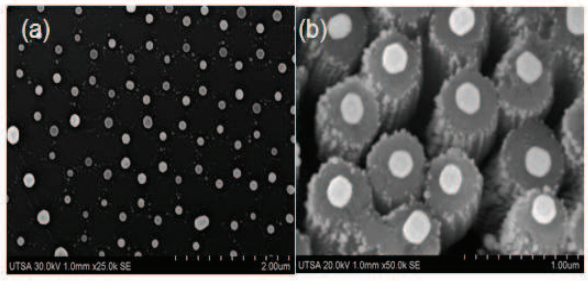


*Fig. 5: The SEM micrographs of 2D ordered Au nanoparticles array in (a) plane Si surface, (b) SiNP array textured surface.*

Fig. 5 depicts two dimensional Au nanoparticles array with the precise array pith fabricated by annealing thin Au film patterned by NSL technique at 850$^0$C for 2 hours in plane Si surface (a) and nanopillar textured Si surface (b), respectively. The measured reflectivity of the Au nanoparticles decorated SiNP textured sample is plotted in Fig. 6 below. The presence of Au nanoparticles is found to be promising for the broad band antireflection effects.

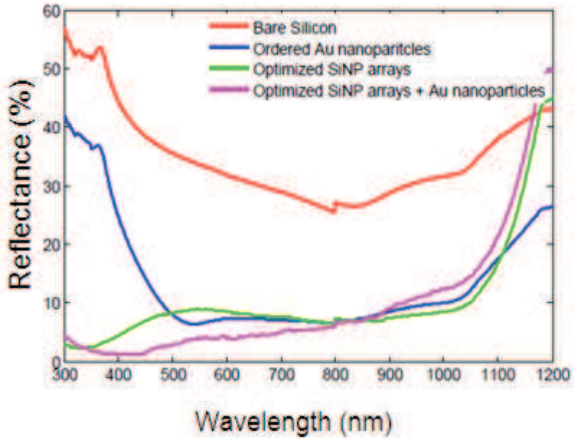


*Fig. 6: Optical reflectance spectra of plane and napillars textured sample with and without Au nanoparticles.*

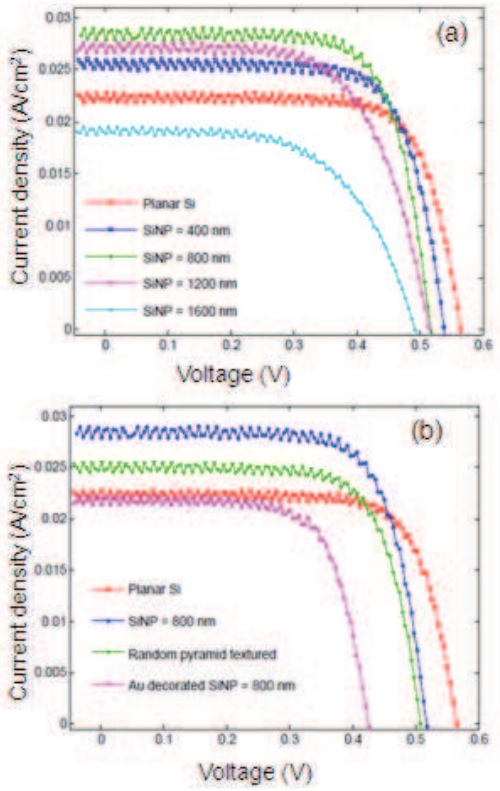


*Fig. 7: Illuminated I-V curves for (a) different solar cells having different SiNP heights, (b) comparison with different solar cells structures.*

*Table 1: Measured illuminated I-V characteristics of different Solar cells.*

| Cells types | $V_{oc}$ (mV) | $J_{sc}$(mA/ $cm^2$) | *FF (%)* | *PCE (%)* | $R_s$ *(ohm)* |
|---|---|---|---|---|---|
| Planar | 574 | 22.4 | 67.95 | 8.65 | 5.9 |
| Random Textured | 517 | 25.5 | 66.82 | 8.76 | 6.2 |
| SiNP 400nm | 547 | 25.9 | 68.21 | 9.58 | 5.3 |
| SiNP 800nm | 527 | 28.9 | 69.93 | 10.7 | 4.7 |
| SiNP 1200nm | 524 | 27.5 | 61.55 | 8.89 | 7.3 |
| SiNP 1600nm | 498 | 19.5 | 56.62 | 5.53 | 9.4 |
| Au decorated SiNP 800nm | 435 | 22.2 | 75.91 | 7.31 | 1.3 |

The measured illuminated *I-V* characteristics of the SiNP array textured solar cells with different pillar heights are presented in Fig. 7(a). The comparison of illuminated *I-V* characteristics for different solar cells with random textured, nanopillars textured and Au nanoparticles decorated nanopillars textured surfaces are plotted in Fig. 7(b). The solar cells parameters such as open circuit voltage ($V_{oc}$), short circuit current density *($J_{sc}$)*, fill factor *(FF)*, power conversion efficiency *(PCE)* and series resistance *($R_s$)* for different solar cells are presented in Table 1. Among the entire SiNP array textured samples, the sample with nanopillar height 800nm has shown the best electrical performance with the power conversion efficiency of 10.7%. The samples with the nanopillars heights greater than 800nm have shown the poor electrical performance. The *Voc, Jsc, FF PCE* all decreases with the increase in nanopillar height due to the increase front surface recombination and poor electrical contacts. When the sample with SiNP height 800nm is decorated by Au nanoparticles then the *PCE* value is decreased by 3.39% (absolute) mainly due to the decreased *Voc* and *Jsc* despite its higher *FF* due to reduced sheet resistance. This suggests that an effective surface passivation is inevitable to reduce surface recombination for the better electrical performance for Au decorated SiNP arry textured sample.

## CONCLUSION

We have demonstrated a simple MAECE process for the fabrication of highly order two dimensional SiNP array for better broad band antireflection effect. SiNP array textured solar cells were fabricated by the processes with the potential for lower cost. The *PCE* value of the optimized radial p-n junction SiNP array textured solar cell was 10.7% which is ~2.0% (absolute) greater than its counterpart planar and random pyramid surface textured solar cells. Au decorated SiNP array textured solar cell depicts the poor electrical performance despite its better antireflection effect due to increase surface recombination, which can improve by effective surface passivation.

## REFERENCES


[1] Cao L. *et al.* 2009 Engineering light absorption in semiconductor nanowire devices, *Nature Matt*. **8** 643-647.

[2] Han S. E. and Chen G. 2010 Optical Absorption Enhancement in Silicon Nanohole Arrays for Solar Photovoltaics, *Nano Letts.* **10** 1012-1015.

[3] Green M. A. and Pillai S. 2012 Harnessing plasmonics for solar cells, *Nature Photonics,* **6** 130-132.

[4] Nakayama K. *et al.* 2008 Plasmonic nanoparticle enhanced light absorption in GaAs solar cells, *Appl. Phys. Letts.* **93** 121904.

[5] Yang Y. *et al. 2012* Enhanced light trapping for high efficiency crystalline solar cells by the application of rear surface plasmons, *Solar Energy Materials and Solar Cells,* **101** 217-226, 2012.

[6] Pudasaini P. R. and Ayon A. 2012 Nanostructured thin film silicon solar cells efficiency improvement using gold nanoparticles, *phys stat. sol. (a),* **209** 1475-1480.

[7] Kim D. R. *et al. 2011* Hybrid Si Microwire and Planar Solar Cells: Passivation and Characterization *Nano Letts.* **11** 2704-2708.

[8] Garnett E. C. and Yang P. 2008 Silicon nanowire radial p-n junction solar cells *J. Am. Chem. Soc.* **130** 9224-9225.

[9] Kim J. *et al.* 2011 Au/Ag bilayered metal mesh as a Si etching catalyst for controlled fabrication of Si nanowires *J. Am. Chem. Soc.* **5** 3222-3229.

[10] Chartier C. *et al.* 2008 Metal-assisted chemical etching of silicon in HF–H2O2 *Electrochimica Acta,* **53** 5509-5516.